A&A 493, 623–628 (2009)
DOI: 10.1051/0004-6361:200810792

Astronomy & Astrophysics

Electron-cyclotron maser emission by power-law electrons in coronal loops

J. F. Tang[1,2] and D. J. Wu[1]

[1] Purple Mountain Observatory, 2 West Beijing Road, Nanjing 210008, PR China
e-mail: jftang@pmo.ac.cn
[2] Graduate School of Chinese Academy of Sciences, Beijing 100039, PR China

Received 13 August 2008 / Accepted 15 October 2008

ABSTRACT

Context. The electron-cyclotron maser (ECM) instability is an important mechanism that amplifies electromagnetic radiation directly by nonthermal electrons trapped in magnetic fields. The nonthermal electrons frequently have a negative power-law distribution with a lower energy cutoff (E_c), which will depress the instability.

Aims. In this paper, it is shown that the lower energy cutoff behavior of power-law electrons trapped in coronal loops can drive the ECM instability efficiently.

Methods. Based on the dispersive relation for high-frequency waves and distribution function for power-law electrons with a lower energy cutoff in a coronal loop, the growth rates of the O and X mode waves at fundamental and harmonic frequencies are calculated.

Results. The results show that the instability is driven when $\delta > \alpha$ because of a population inversion below the cutoff energy E_c, where δ is the steepness index describing the cutoff behavior and α the power-law spectrum index. The growth rates increase with δ and E_c, but decrease with α, σ, and Ω, where σ is the magnetic mirror ratio of the loop and Ω the ratio frequency in the loop.

Conclusions. This novel driving mechanism for the ECM emission can be expected to have a potential importance for understanding the microphysics of radio bursts from the Sun and others.

Key words. masers – plasmas – radiation mechanisms: nonthermal – Sun: radio radiation

1. Introduction

Solar radio emission has attracted many authors' attention during the past several decades. The key question is how a beam of fast electrons leads to the generation of electromagnetic waves. Ginzburg & Zhelezniakov (1958) are the pioneers in this field by advancing a theory to explain the observed fundamental (F) and harmonic (H) bands. Goldman (1983) also discussed this topic in subsequent years. Cairns (1987a–c), Robinson et al. (1993, 1994), Willes et al. (1996), Robinson & Cairns (1998a–c), Wu et al. (1994), and Yoon (1995, 1997, 1998) all put forward the plasma emission theory to explain the fundamental and harmonic emission in type III solar radio bursts. In this conventional theory, Langmuir waves that resulted from fast electrons play a pivotal role and are partly converted into electromagnetic waves by nonlinear wave-wave interaction. This model also incorporates large-angle scattering and reabsorption of fundamental emission amid ambient density fluctuations in the corona and solar wind. They all assume that the ambient magnetic field of the source regions of type III bursts is very weak. Although this approximation may be justified for source regions far enough away from the Sun, it is not obvious that it is appropriate for the emissions taking place near an active region in the low corona where nonthermal electrons are trapped by strong magnetic fields and are the main emitting sources of solar microwave bursts and spikes.

Another important theory was proposed by Wu & Lee (1979). In this model, radio emissions are produced by direct amplification of electromagnetic waves at the frequencies near the electron gyrofrequency and its harmonics. The ECM instability is the direct amplification mechanism for radio emissions in magnetized plasmas. With this theory, they can explain Earth's auroral kilometric radiation well. In recent years, Wu et al. (2002, 2004, 2005), Chen et al. (2002), and Yoon et al. (2002) further developed this mechanism and applied it to explain type III solar radio bursts. In accordance with their model, amplified waves propagate in a magnetic flux tube until they arrive at a point where the frequencies of the excited waves are equal to the local exterior cutoff frequency. With some simplified models of magnetic field and electron density, some long-standing problems about type III solar radio bursts have been accounted for.

Most discussions of the ECM instability suppose that the nonthermal electrons have a loss-cone distribution, in which the perpendicular population inversion in electron energy is effective for driving the ECM instability (Chen et al. 2002). Observations from the hard X-ray, however, demonstrate that nonthermal flare-electrons approximately have a negative power-law distribution with a lower energy cutoff E_c (Lin 1974; Gan et al. 2001), which will depress the growth rates of the instability. The cyclotron radiation from these power-law electrons can be regarded as the main source of microwave bursts in the GHz band (Kundu & Vlahos 1982; Aschwanden 2002; Stupp 2000; Fleishman 2004; Wu et al. 2007). In a recent work, Wu & Tang (2008) argue that the lower energy cutoff behavior of power-law electrons can drive the ECM instability efficiently even if the nonthermal electrons have an isotropic distribution.

In this paper, we apply this driving mechanism by the cutoff behavior to cases of coronal loops, where nonthermal electrons have an anisotropic distribution. The results show that the growth rates of waves in the ordinary (O) and extraordinary (X) modes at the fundamental and harmonic frequencies increase with the steepness index δ of the cutoff behavior and the cutoff energy E_c of the electron distribution function, but decrease with the power-law spectrum α of the distribution function and the magnetic-mirror ratio σ and the ratio frequency (the electron gyrofrequency to the plasma frequency) Ω of the magneto-loop plasma.

This paper is organized as follows. In Sect. 2 we discuss the lower energy cutoff behavior of power-law electrons trapped in magneto-loops and introduce the distribution function. Then, the theory calculating the growth rate of the ECM instability is described in Sect. 3. The calculating results of the growth rates for the waves in the O and X modes at the fundamental and harmonic frequencies are discussed in Sect. 4. Finally, the summary and conclusions are presented in Sect. 5.

2. Lower energy cutoff of power-law electrons

According to a thick-target interaction mode (Brown 1971), the bremsstrahlung radiation of the power-law electrons caused by their interaction with the solar atmosphere also results in a power-law spectrum in the hard X-ray band, but with a different spectrum index. Thus, the electron spectrum index can be deduced from the observed hard X-ray spectrum. However, it is very difficult to determine a special form for the lower-energy cutoff behavior of a power-law electron event based on observations. Gan et al. (2001) discussed the two extreme cases of sharp and saturation cutoffs. In order to fit more general cases, we introduce the hyperbolic tangent function with two parameters (i.e., the cutoff energy E_c and the steepness index δ) to describe the lower energy cutoff behavior of power-law energy spectrum (Wu & Tang 2008). The resulting energy distribution for the beam electrons has form

$$F_b(E) = A_b\,(E/E_c)^{-\alpha}\tanh\,(E/E_c)^{\delta}\,, \tag{1}$$

where α is the spectrum index of power-law electrons, E the kinetic energy of nonthermal electrons, and A_b the normalization factor determined by $\int_0^\infty F_b(E)\mathrm{d}E = 1$. As pointed out by Wu & Tang (2008), the power-law electrons with the steepness cutoff behavior of $\delta > \alpha$ can efficiently drive the ECM instability, even if the nonthermal electrons have an isotropic distribution.

In coronal magnetic loops, however, the distribution of nonthermal electrons in velocity space, in general, is anisotropic due to the strongly magnetic confinement. Stupp (2000) and Fleishman (2004) discuss, respectively, the saturation length and the natural spectral bandwidth of the ECM emission by the power-law electrons with a loss-cone angular distribution. For the magnetic loop case, Zaitsev et al. (1997) also discussed the radiation of the power-law electrons with a loss-cone distribution, but for the radiation in the Z mode. In particular, Zaitsev et al. (1997) introduced the magnetic mirror ratio parameter ($\sigma = B_{\max}/B_{\min}$) in their distribution function to take the magnetic mirror effect of the magnetic loop into account, where $B_{\max}$ and $B_{\min}$ are the maximal and minimal magnetic field strengths in the loop, respectively. These authors all used the sharp cutoff condition in their distribution functions for the energy spectrum of the power-law electrons. To fit more general lower energy cutoff behavior, following Wu & Tang (2008) and Zaitsev et al. (1997), we introduce a novel distribution function of the power-law electrons for the coronal loop case as follows:

$$\begin{aligned} F_b &= A\frac{1-\exp\left[(1-\sigma)\,u_\perp^2/u_\parallel^2\right]}{\left(\left(u_\perp^2+u_\parallel^2\right)/\gamma^2\right)^{\alpha+1/2}}\tanh\left(\frac{u_\perp^2+u_\parallel^2}{u_c^2}\right)^{\delta} \\ &= A\Theta(\mu)\frac{1-\exp\left[(1-\sigma)\left(\mu^{-2}-1\right)\right]}{(u/\gamma)^{2\alpha+1}}\tanh\left(\frac{u}{u_c}\right)^{2\delta}, \end{aligned} \tag{2}$$

where $u = (u_\perp^2+u_\parallel^2)^{1/2}$, $\boldsymbol{u}$ momentum per the unit mass, $u_\perp$and $u_\parallel$ are the components of $\boldsymbol{u}$ perpendicular and parallel to the ambient magnetic field. Also, $\gamma = \sqrt{1+u^2/c^2}$ is the the Lorentz factor, $\mu = u_\parallel/u$, and $\Theta(\mu)$ is the Heaviside step function defined by $\Theta(\mu) = 1$ for $0 < \mu \le 1$ and $\Theta(\mu) = 0$ for $-1 \le \mu < 0$, which implies that the nonthermal electrons are in a directed beam along the magnetic field in the loop. Finally, the normalized factor A can be determined by

$$\int\!\!\int\!\!\int F_b(u,\mu)\mathrm{d}^3\boldsymbol{u} = 1. \tag{3}$$

The energy distribution function of the beam electrons, $F_b(E)$, can be obtained by the integral of $F_b(u,\mu)\mathrm{d}\mu$ from -1 to 1, that is,

$$\begin{aligned} F_b(E) &= 2\pi u^2\frac{\mathrm{d}u}{\mathrm{d}E}\int_{-1}^{1}F_b(u,\mu)\mathrm{d}\mu \\ &= A_b\gamma^{2\alpha+2}\,(\gamma+1)^{-\alpha}\,(E)^{-\alpha}\tanh\left(\frac{E}{E_c}\right)^{\delta}, \end{aligned} \tag{4}$$

where the kinetic energy $E = mu^2/(\gamma+1)$, E_c denotes the cutoff energy, the Lorentz factor $\gamma = 1+E/mc^2$, and the normalization factor A_b can be determined by $\int F_b(E)\mathrm{d}E = 1$.

Figure 1 shows a two-dimensional mesh plot of the distribution $F_b(u_\perp, u_\parallel)$ against $u_\perp$ and $u_\parallel$ for different values of the steepness index δ, where the negative power-law spectrum index $\alpha = 3$, and the weakly relativistic condition of $\gamma - 1 = E/mc^2 \ll 1$ has been used, and $F_b(u_\perp, u_\parallel)$ in the plot has been normalized by their maxima. It is clear that the slope becomes steepest when $\delta \gg \alpha$, which corresponds to the sharp cutoff case. And when $\delta \le \alpha$, the slope $\partial F_b/\partial u_\perp$ is negative, which is the saturation cutoff. For general cases of $\delta > \alpha$ the distribution of power-law electrons shows a steepness cutoff behavior (i.e., a positive slope that indicates an energy reversion) just below the cutoff energy E_c if only $E_c \gg T_e$, which is easily satisfied in principle.

3. General formulation for the ECM growth rate

It is generally acknowledged that fast electrons can lead to maser instabilities in magnetized plasmas. We consider that the thermal electrons are dominant in the plasma and the nonthermal electrons that lead to instabilities only occupy a very small component. The dispersion relation is given approximately by the cold-plasma theory (Wu et al. 2002; Chen et al. 2002; Melrose 1986; Melrose et al. 1982; Melrose et al. 1984; Sharma & Vlahos 1984; Yoon et al. 1998; Yoon & Weatherwax 1998):

$$N_q^2 = 1 - \frac{1}{\omega_q\left(\omega_q+\tau_q\Omega\right)}, \tag{5}$$

where $\tau_q = -s_q + q\sqrt{s_q^2+\cos^2\theta}$, $s_q = \omega_q\Omega\sin^2\theta/2\left(\omega_q^2-1\right)$, θ denotes the wave phase angle with respect to the ambient magnetic field, Ω is the electron cyclotron frequency (ω_{ce}) in units

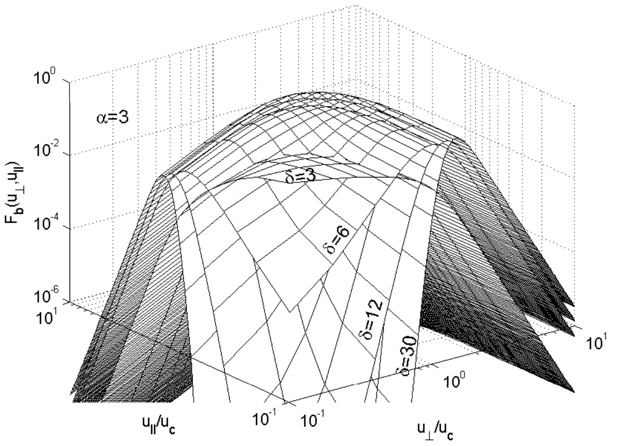

Fig. 1. Lower-energy cutoff behaviors of power-law electrons with spectrum index $\alpha = 3$.

of the plasma frequency $\omega_{\rm p}$, $q = +$, and $q = -$ denotes the O and X modes, respectively, and finally all frequencies have been normalized by $\omega_{\rm p}$.

For the sth harmonic with frequency $\omega \simeq s\Omega$, the growth rate of the ECM instability is given by (see e.g. Chen et al. 2002)

$$\frac{\omega_{qi}}{\omega_{\rm ce}} = \frac{\pi}{2}\frac{n_{\rm b}}{n_0}\int {\rm d}^3\boldsymbol{u}\frac{\gamma\left(1-\mu^2\right)}{\Omega\omega_q\left(1+T_q^2\right)R_q}\delta\left(\gamma - \frac{s\Omega}{\omega_q} - \frac{N_q\mu u}{c}\cos\theta\right) \times\left\{\frac{\omega_q}{\Omega}\left[\gamma K_q\sin\theta + T_q\left(\gamma\cos\theta - \frac{N_q\mu u}{c}\right)\right]\frac{J_s(b_q)}{b_q} + J_s'(b_q)\right\}^2\left[u\frac{\partial}{\partial u} + \left(\frac{N_q u\cos\theta}{c\gamma} - \mu\right)\frac{\partial}{\partial\mu}\right]F_{\rm b}(u,\mu) \tag{6}$$

with

$$b_q = N_q\frac{\omega_q}{\Omega}\frac{u}{c}\sqrt{1-\mu^2}\sin\theta,$$

$$R_q = 1 - \frac{\Omega\tau_q}{2\omega_q\left(\omega_q+\tau_q\Omega\right)^2}\left(1 - \frac{qs_q}{\sqrt{s_q^2+\cos^2\theta}}\frac{\omega_q^2+1}{\omega_q^2-1}\right),$$

$$K_q = \frac{\Omega\sin\theta}{\left(\omega_q^2-1\right)\left(\omega_q+\tau_q\Omega\right)}, \qquad T_q = -\frac{\cos\theta}{\tau_q}, \tag{7}$$

where n_0 and $n_{\rm b}$ are the electron number densities of the ambient plasma and nonthermal component, respectively, $J_s(b_q)$ is the Bessel function of the first kind, with the prime denoting the derivative with respect to the argument, and the Dirac function $\delta(\gamma - s\Omega/\omega_q - N_q u\mu\cos\theta/c)$ implies the resonant condition.

In general, the nonthermal electrons that are responsible for solar microwaves and hard X ray emissions have typical energy of tens of keV (Lin 1974; Gan et al. 2001), that is, they are weakly relativistic in energy. This allows the weakly relativistic approximation $\gamma \simeq 1$ to be used for the nonthermal electrons in above integral. For the resonant condition in the Dirac function, however, including weakly relativistic effects is necessary because the relativistic effect in the resonant condition, even in the very weakly relativistic case, has a decisive effect on the efficiency of the amplification of the emitted wave (Wu & Lee 1979). In the weakly relativistic case of $\gamma - 1 \ll 1$, the Lorentz factor may been taken as $\gamma \simeq 1 + u^2/2c^2$ in the resonant condition. This leads to the resonant momentum as follows:

$$\frac{u_{{\rm r}l}}{c} = N_q\mu\cos\theta + l\sqrt{N_q^2\mu^2\cos^2\theta + 2\left(\frac{s\Omega}{\omega}-1\right)}, \tag{8}$$

where, $l = \pm$ denotes the two roots of the resonant condition and u_{r-} is present only when $\theta < 90°$ and $s\Omega < \omega_q$. Finally, to integrate Eq. (6) over the momentum u we obtain the growth rate

$$\frac{\omega_{qi}}{\omega_{\rm ce}} = \frac{\pi^2}{\Omega\omega_q}\frac{n_{\rm b}}{n_0}\frac{c}{\left(1+T_q^2\right)R_q}\int_0^1{\rm d}\mu\frac{1-\mu^2}{\sqrt{N^2\mu^2\cos^2\theta + 2\left(s\Omega/\omega - 1\right)}} \times\sum_{l=\pm}u_{{\rm r}l}^2\left\{\frac{\omega_q}{\Omega}\left[K_q\sin\theta + T_q\left(\cos\theta - \frac{N_q u_{{\rm r}l}\mu}{c}\right)\right]\frac{J_s(b_{{\rm r}l})}{b_{{\rm r}l}} + J_s'(b_{{\rm r}l})\right\}^2\left[u_{{\rm r}l}\frac{\partial}{\partial u} + \left(\frac{N_q u_{{\rm r}l}\cos\theta}{c} - \mu\right)\frac{\partial}{\partial\mu}\right]F_{\rm b}(u_{{\rm r}l},\mu). \tag{9}$$

4. Discussions of the ECM growth rate

The growth rate of the emission wave in the O and X modes can be calculated on the basis of the integral of Eq. (9) with the distribution $F_{\rm b}$ given by Eq. (2). For the given nonthermal electron parameters (δ, α and $E_{\rm c}$) and the ambient magneto-plasma parameters (Ω and σ) in the coronal loop, the growth rate depends on two variables (ω_q, θ). By peak growth rate, we mean the growth rate with highest magnitude as a function of one variable while the other is fixed. In contrast, the highest value in both (ω_q, θ) is called the maximum growth rate. We first discuss the dependence of the growth rate on the lower energy cutoff behavior, that is, on the steepness index δ and the cutoff energy $E_{\rm c}$. As an illustrative case, Fig. 2 shows the peak growth rates calculated by varying the frequency ω_q for a given wave phase angle θ, where panels O_1 and O_2 are the fundamental ($s = 1$) and harmonic ($s = 2$) waves in the O mode, panels X_1 and X_2 are the fundamental and harmonic waves in the X mode, and different curves are for different steepness indices $\delta = 3$, 4, 5, 6, and 7 but a given spectrum index $\alpha = 3$ and cutoff energy $E_{\rm c} = 20$ keV. The ambient plasma parameters $\Omega = 3.34$ and $\sigma = 10$ have been used and the growth rate ω_i normalized by $\omega_{\rm ce}n_{\rm b}/n_0$ in Fig. 2.

From Fig. 2, one can find that the growth rates are all negative for the saturation case of $\delta \le \alpha = 3$ (the harmonic-wave growth rates for the O and X modes are negative, too, but not present in panels O_2 and X_2). For general steepness cases of $\delta > \alpha$, the growth rates of the X mode waves (X_1 and X_2) are considerably higher than those of the O mode waves (O_1 and O_2). For the O mode, the growth rate of harmonic waves (O_2) is much less than for fundamental waves (O_1) and is only ~2% of O_1, but in the X mode the growth rate of harmonic waves (X_2) is slightly lower than that of fundamental waves (X_1) by a factor ~1.5. In particular, it is worth noticing that these growth rates all increase with the steepness index δ. This implies that the steepness cutoff behavior with a positive slope (i.e., $\partial F_{\rm b}/\partial E > 0$) of power-law electrons indeed can efficiently excite the ECM instability. Moreover, the steeper cutoff behavior (i.e., with a larger steepness index δ) more easily excites the ECM instability. For the case of the saturation cutoff of $\delta \le \alpha$, however, power-law electrons cannot excite the ECM instability because of the absence of population inversion.

In Fig. 2, it is also clearly shown that the growth rates in the four modes (O_1, O_2, X_1, and X_2) all reach the maximum values at the direction close to perpendicular to the ambient magnetic field (i.e., $\theta \simeq \pi/2$). Figure 3 plots the maximum growth rates as a function of the cutoff energy $E_{\rm c}$, where the parameters $\alpha = 3$, $\delta = 4$, $\Omega = 3.34$, $\sigma = 10$, and $\theta = 1.58$ have been used. From Fig. 3, it is clear that the growth rates all increase with the cutoff energy $E_{\rm c}$. It is found, again, that the growth rates of the X mode waves are considerably higher than those of the O mode waves and that the growth rate of O_2 is much lower than those of the

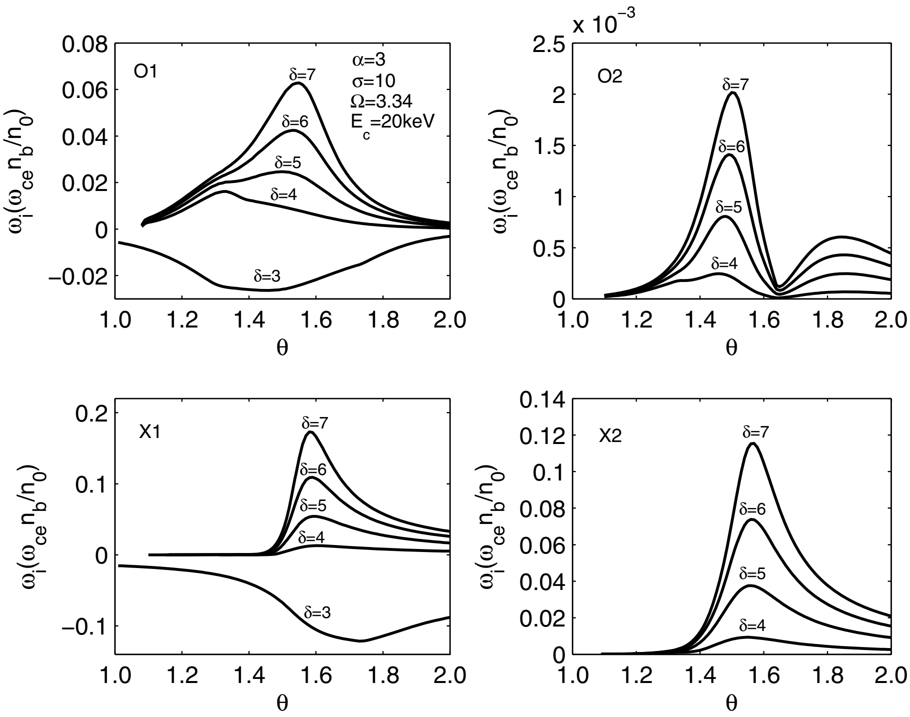

Fig. 2. Peak growth rates driven by the ECM instability: O_1, fundamental waves in the O mode; O_2, harmonic waves in the O mode; X_1, fundamental waves in the X mode; X_2, harmonic waves in the X mode.

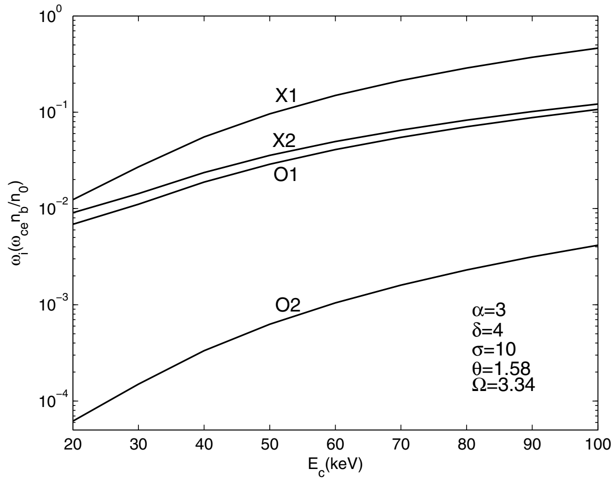

Fig. 3. Maximum growth rates versus the cutoff energy E_c: O_1, fundamental waves in the O mode; O_2, harmonic waves in the O mode; X_1, fundamental waves in the X mode; X_2, harmonic waves in the X mode.

other three modes. It should be pointed out, however, that the X_1 emission cannot escape from its astrophysical source, although it has the highest growth rate because its emitting frequency, $\omega_- \simeq \Omega$, is always below the cutoff frequency for the X mode, $\Omega_{XC} \simeq \sqrt{\Omega^2/4+1}+\Omega/2$. In consequence, the dominating modes are in reality the X_2 and O_1 emissions, which have growth rates very close for a wide range of E_c.

Next we consider the dependence of the growth rate on the spectrum index α of power-law electrons. Figure 4 plots the peak growth rates versus the wave phase angle θ, where panels are denoted in the same way as in Fig. 2, but different curves are for different spectrum indices $\alpha = 2, 3, 4, 5$, and 6 and a given steepness index $\delta = 6$ and cutoff energy $E_c = 20$ keV. The ambient plasma parameters $\Omega = 3.34$ and $\sigma = 10$ have been used, too. From Fig. 4, one can find, again, that the growth rates all are negative for the saturation case of $\alpha = \delta = 6$. The harmonic-wave growth rates for the O and X modes are negative, too, but not present in the panels O_2 and X_2. For general steepness cases of $\alpha < \delta$, the growth rates all decrease with the spectrum index α. This indicates that the negative power-law spectrum of energetic electrons will depress the ECM instability and that a softer spectrum (i.e., with a larger spectrum index α) leads to a lower growth rate.

Finally, we discuss the dependence of the growth rate on the ambient plasma parameters, the ratio-frequency $\Omega = \omega_{ce}/\omega_p$, and the magnetic mirror-ratio $\sigma = B_{max}/B_{min}$. Figure 5 presents the peak growth rates varying with the wave phase angle θ, where panels are denoted in the same way as above, and different curves are for different ratio-frequencies $\Omega = 2, 3.34, 5$, and 10 but given other parameters $\alpha = 3$, $\delta = 4$, $E_c = 20$ keV, and $\sigma = 10$. The result shows that, with Ω decreasing, the growth rates become higher and the unstable range of θ wider except for the X_1 mode that cannot escape from its astrophysical source region. In Fig. 5, the curve with $\Omega = 10$ for the O_2 mode does not present in the panel O_2 because its growth rate is too low.

Figure 6 presents the dependence of the mirror-ratio σ in the coronal loop on the growth rates, where the parameters $\alpha = 3$, $\delta = 4$, $E_c = 20$ keV, $\Omega = 3.34$, and $\theta = 1.58$ have been used. From Fig. 6, one can find that the growth rates all decrease with σ. In particular, the growth rates are sensitive to the mirror ratio for small mirror ratios of $\sigma < 5$ and decrease rapidly with σ, but for high mirror-ratios of $\sigma > 10$ the growth rates approach constants. By the way, as denoted in the curve of O_2, the growth rate of the O_2 mode has been enlarged by a factor of 50 because of how low it is.

5. Summary and conclusions

The ECM instability, which can be driven by nonthermal electrons trapped in magnetic fields, is an important radiation mechanism in astrophysics and has been extensively applied to various short-time radio-burst phenomena, such as the auroral kilometric radiation from the Earth, radio emission from other magnetized planets (e.g. Jupiter and Saturn) in the solar

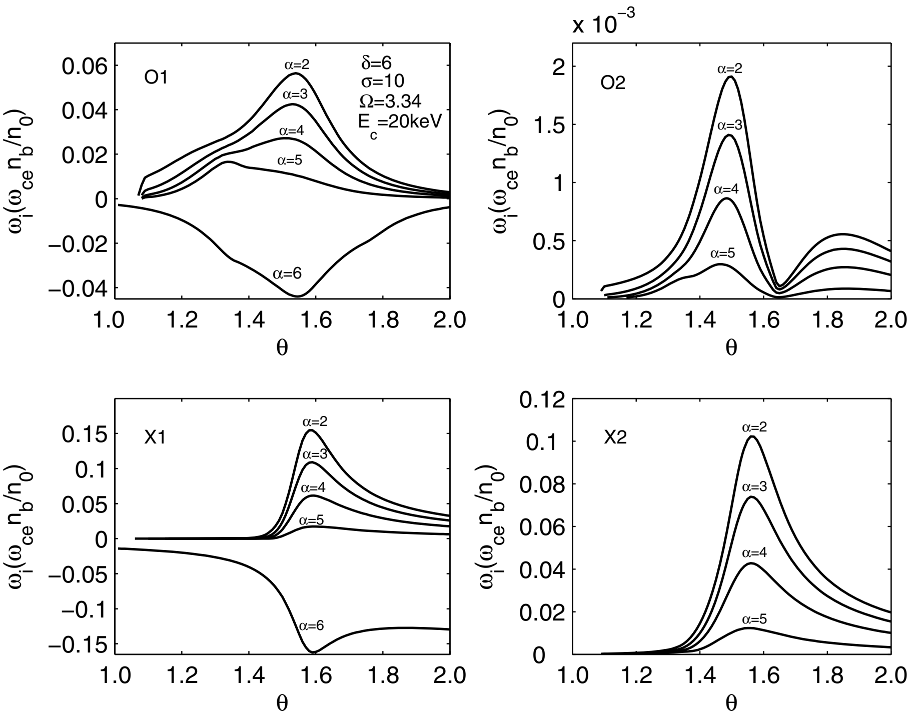

Fig. 4. Peak growth rates driven by the ECM instability: O_1, fundamental waves in the O mode; O_2, harmonic waves in the O mode; X_1, fundamental waves in the X mode; X_2, harmonic waves in the X mode.

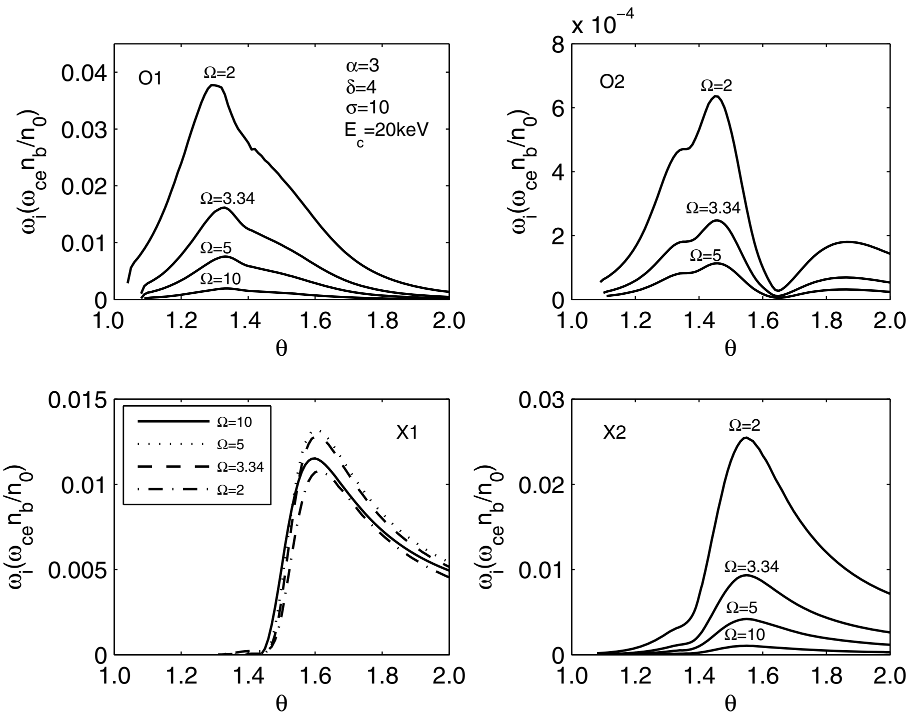

Fig. 5. Peak growth rates driven by the ECM instability: O_1, fundamental waves in the O mode; O_2, harmonic waves in the O mode; X_1, fundamental waves in the X mode; X_2, harmonic waves in the X mode.

system and extrasolar planets, radio bursts or spikes from the Sun and other stars, and the time-varying emission from blazar jets (see Treumann 2006, for a recent review). Astrophysical observations, on the other hand, demonstrate that nonthermal electrons frequently present in a power-law distribution with a lower-energy cutoff. In this paper, we investigated the growth rates of the ECM emissions of fundamental and harmonic waves in the O and X modes driven by power-law electrons trapped in coronal magneto-loops. The trapped power-law electrons may have a loss-cone distribution due to the magnetic mirror-force effect of the loop magnetic field on the power-law electrons. We introduced a new distribution function of power-law electrons that describes not only a continual and smooth loss-cone boundary but also a continual and smooth lower energy cutoff behavior. Based on the weakly relativistic approximation, we discussed the dependence of the growth rates on the parameters of both the power-law electrons and the ambient magneto-plasma in the coronal loop.

Results from our calculations show that the power-law electrons with the steepness cutoff (i.e., $\delta > \alpha$) can excite the ECM instability efficiently because of the energy reverse distribution just below the cutoff energy E_c, and the growth rates of

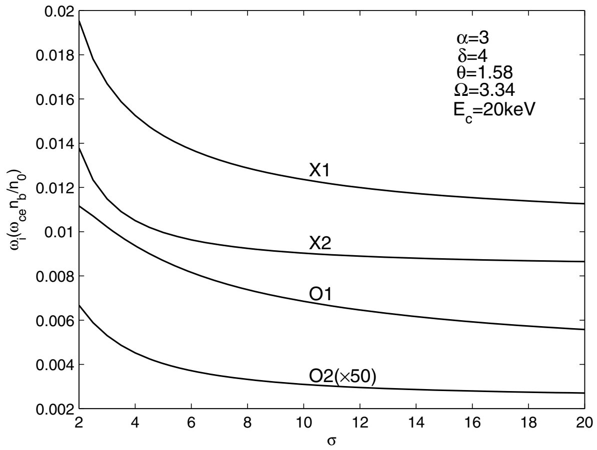

Fig. 6. Plots maximum growth rates versus the mirror ratio σ: O_1, fundamental waves in the O mode; O_2, harmonic waves in the O mode; X_1, fundamental waves in the X mode; X_2, harmonic waves in the X mode.

fundamental and harmonic waves in both the O and X modes all increase with both the steepness index δ and the cutoff energy E_c. Also the results show that the X_2 and O_1 mode waves dominate the radiation driven by the ECM instability. On the other hand, for the saturation cutoff case of $\delta \le \alpha$, the power-law electrons cannot drive the ECM instability because of the absence of population inversion.

We also discussed the dependence of the growth rate on the spectrum index α. The result indicates that the negative power-law spectrum of nonthermal electrons will depress the growth rate of the ECM instability and that a softer spectrum (i.e., with a larger spectrum index α) leads to a lower growth rate.

Finally, the growth rate of the ECM instability sensitively depends on the ambient magneto-plasma parameters too, the ratio-frequency $\Omega = \omega_{ce}/\omega_p$, and the magnetic mirror-ratio $\sigma = B_{max}/B_{min}$ in the coronal loop. The result shows that, with Ω decreasing, the growth rates become larger and the unstable range of θ wider except for the X_1 mode that cannot escape from its astrophysical source region. On the other hand, the growth rates decrease rapidly with σ for low mirror ratios of $\sigma < 5$, but approach constants for high mirror ratios of $\sigma > 10$.

Acknowledgements. This work is supported by NSFC grant 10425312 and 40574065, by 973 program 2006CB806302, and by CAS grant KJCX2-YW-T04. Also the authors are grateful to the anonymous referee for valuable comments.

References

Aschwanden, M. J. 2002, Space Sci. Rev., 101, 1
Brown, J. C. 1971, Sol. Phys., 18, 489
Cairns, I. H. 1987a, J. Plasma Phys., 38, 169
Cairns, I. H. 1987b, J. Plasma Phys., 38, 179
Cairns, I. H. 1987c, J. Plasma Phys., 38, 199
Chen, Y. P., Zhou, G. C., Yoon, P. H., & Wu, C. S. 2002, Phys. Plasmas, 9, 2816
Fleishman, G. D. 2004, Astron. Lett., 30, 603
Gan, W. Q., Li, Y. P., & Chang, J. 2001, ApJ, 552, 858
Ginzburg, V. L., & Zheleznıakov, V. V. 1958, Soviet Astron., 2, 653
Goldman, M. V. 1983, Sol. Phys., 89, 403
Kundu, M. R., & Vlahos, L. 1982, Space Sci. Rev., 32, 405
Lin, R. P. 1974, Space Sci. Rev., 16, 189
Melrose, D. B. 1986, Instabilities in Space and Laboratory Plasmas (New York: Cambridge Univ. Press)
Melrose, D. B., Hewitt, R. G., & Ronnmark, K. G. 1982, J. Geophys. Res., 87, 5140
Melrose, D. B., Dulk, G. A., & Hewitt, R. G. 1984, J. Geophys. Res., 89, 897
Robinson, P. A., & Cairns, I. H. 1998a, Sol. Phys., 181, 363
Robinson, P. A., & Cairns, I. H. 1998b, Sol. Phys., 181, 395
Robinson, P. A., & Cairns, I. H. 1998c, Sol. Phys., 181, 429
Robinson, P. A., Willes, A. J., & Cairns, I. H. 1993, ApJ, 408, 720
Robinson, P. A., Cairns, I. H., & Willes, A. J. 1994, ApJ, 422, 870
Sharma, R. R., & Vlahos, L. 1984, ApJ, 280, 405
Stupp, A. 2000, MNRAS, 311, 251
Treumann, R. A. 2006, Astron. Astrophys. Rev., 13, 229
Willes, A. J., Robinson, P. A., & Melrose, D. B. 1996, Phys. Plasmas, 3, 149
Wu, C. S., & Lee, L. C. 1979, ApJ, 230, 621
Wu, C. S., Yoon, P. H., & Zhou, G. C. 1994, ApJ, 429, 406
Wu, C. S., Wang, C. B., Yoon, P. H., Zheng, H. N., & Wang, S. 2002, ApJ, 575, 1094
Wu, C. S., Reiner, M. J., Yoon, P. H., Zheng, H. N., & Wang, S. 2004, ApJ, 605, 503
Wu, C. S., Wang, C. B., Zhou, G. C., Wang, S., & Yoon, P. H. 2005, ApJ, 621, 1129
Wu, D. J., & Tang, J. F. 2008, ApJ, 677, L125
Wu, D. J., Huang, J., Tang, J. F., & Yan, Y. H. 2007, ApJ, 665, L171
Yoon, P. H. 1995, Phys. Plasmas, 2, 537
Yoon, P. H. 1997, Phys. Plasmas, 4, 3863
Yoon, P. H. 1998, Phys. Plasmas, 5, 2590
Yoon, P. H., & Weatherwax, A. T. 1998, Geophys. Res. Lett., 25, 4461
Yoon, P. H., Weatherwax, A. T., & Rosenberg, T. J. 1998, J. GeoPhys. Res., 103, 4071
Yoon, P. H., Wu, C. S., & Wang, C. B. 2002, ApJ, 576, 552
Zaitsev, V. V., Kruger, A., Hildebrandt, J., & Kliem, B. 1997, A&A, 328, 390